Novel targeted deregulation of c-Myc cooperates with Bcl-X_L to cause plasma cell neoplasms in mice

Wan Cheung Cheung,[1] Joong Su Kim,[2] Michael Linden,[3] Liangping Peng,[2] Brian Van Ness,[3] Roberto D. Polakiewicz,[1] and Siegfried Janz[2]

[1]Cell Signaling Technology Inc., Beverly, Massachusetts, USA. [2]Laboratory of Genetics, Center for Cancer Research, National Cancer Institute, NIH, Bethesda, Maryland, USA. [3]University of Minnesota, Minneapolis, Minnesota, USA.

Deregulated expression of both Myc and Bcl-X_L are consistent features of human plasma cell neoplasms (PCNs). To investigate whether targeted expression of Myc and Bcl-X_L in mouse plasma cells might lead to an improved model of human PCN, we generated Myc transgenics by inserting a single-copy histidine-tagged mouse *Myc* gene, Myc^{His}, into the mouse Ig heavy-chain Cα locus. We also generated Bcl-X_L transgenic mice that contain a multicopy Flag-tagged mouse $Bcl\text{-}x^{Flag}$ transgene driven by the mouse Ig κ light-chain 3′ enhancer. Single-transgenic Bcl-X_L mice remained tumor free by 380 days of age, whereas single-transgenic Myc mice developed B cell tumors infrequently (4 of 43, 9.3%). In contrast, double-transgenic Myc/Bcl-X_L mice developed plasma cell tumors with short onset (135 days on average) and full penetrance (100% tumor incidence). These tumors produced monoclonal Ig, infiltrated the bone marrow, and contained elevated amounts of Myc^{His} and Bcl-X_L^{Flag} proteins compared with the plasma cells that accumulated in large numbers in young tumor-free Myc/Bcl-X_L mice. Our findings demonstrate that the enforced expression of Myc and Bcl-X_L by Ig enhancers with peak activity in plasma cells generates a mouse model of human PCN that recapitulates some features of human multiple myeloma.

Introduction

Plasma cell neoplasms (PCNs) in humans comprise multiple myeloma (MM), Ig deposition and heavy-chain diseases, and plasmacytoma (PCT), which occurs as solitary PCT of bone and extramedullary PCT. Several mouse models of human PCN have been developed to study mechanisms of neoplastic plasma cell development and design new strategies for tumor treatment and prevention. Established mouse models of human PCN include tumors that arose spontaneously in old C57BL/KaLwRij mice and that resemble human MM (reviewed in ref. 1), peritoneal PCT that can be induced in strain BALB/c by intraperitoneal injections of proinflammatory agents and further accelerated by infection of mice with transforming retroviruses (reviewed in ref. 2), and the transplantation of human MM cells into SCID mice that harbor preimplanted human fetal bone as a nesting ground for the tumor cells (3–5). Currently emerging mouse models of human PCN are based on transgenic expression in B cells of IL-6 (6) and NPM-ALK (7) (fusion protein of nucleophosmin and anaplastic lymphoma kinase), or viral transduction of NPM-ALK in bone marrow cells (8). While all of these models afford valuable insights into the biology of human PCN, many important features of human PCN have not been adequately recapitulated in mice. One such feature with profound implications for pathogenesis, treatment, and prevention of human PCN is the collaboration of deregulated *Myc* (c-*Myc*) with tumor suppressor genes of the *Bcl-2* family.

Deregulated expression of *Myc* is a consistent feature of PCN in humans and mice. In human MM, *Myc* appears to be activated in *trans* by a variety of signaling pathways converging at the *Myc* promoter (9, 10), possibly including IL-6 via Stat3 (11). Increased translation of *Myc* mRNA due to mutations in *Myc*'s internal ribosome entry site (12), stabilization of Myc protein via Ras (13) and other signaling pathways (14, 15), and chromosomal translocations deregulating *Myc* (16–18) may further contribute to *Myc* overexpression in MM. Upregulation of *Myc* may be of prognostic significance for MM patients (10). In contrast to human MM, the mechanism of *Myc* activation in BALB/c mouse PCT is uniform and well defined. Virtually all of these tumors harbor chromosomal translocations (19, 20) that activate *Myc* (21) by joining the *Myc-Pvt1* locus at 15D1 with the Ig heavy-chain locus *Igh* at 12F2 or one of the Ig light-chain loci, *Igκ* at 6C1 or *Igλ* at 16A3, resulting in T(12;15)(*Igh-Myc*), T(6;15)(*Igκ-Pvt1*), and T(15;16)(*Pvt1-Igλ*), respectively. The most common translocation (~90%) is T(12;15), which juxtaposes *Myc* in approximately 85% of T(12;15)-harboring tumors to the most downstream *Igh* gene, Cα. Mimicking the *Myc-Igh*(Cα) juxtaposition by gene insertion in mice might result in a mode of *Myc* deregulation that is conducive to plasmacytomagenesis and modeling of human PCN in mice.

Upregulation of death suppressor genes of the *Bcl-2* family is another consistent feature of human and mouse PCN. Human MMs exhibit low levels of Bcl-2, but high levels of Mcl-1 and Bcl-X_L (22), the main survival factors in MM (23–26). Overexpression of Bcl-X_L via Stat3, a possible prognostic factor in MM (27), may be involved in growth factor independence of MM. In mouse PCT (28) and normal plasma cells in mice (29, 30), Bcl-X_L, Bcl-2, and A1, rather than Mcl-1, are the main survival genes. The critical role of Bcl-X_L in survival control of human MM and mouse PCT suggests that the enforced expression of this Bcl-2 family

Nonstandard abbreviations used: multiple myeloma (MM); National Cancer Institute (NCI); plasma cell neoplasm (PCN); plasmacytoma (PCT).

Conflict of interest: The authors have declared that no conflict of interest exists.

Citation for this article: *J. Clin. Invest.* **113**:1763–1773 (2004). doi:10.1172/JCI200420369.

member is particularly promising for modeling of human PCN in mice. Studies on the biology of Bcl-X_L and insights from transgenic mice expressing Bcl-X_L (31), Bcl-2 (32, 33), Mcl-1 (34), or A1 (35) in B cells support this proposition. In mature B cells, Bcl-X_L is upregulated in response to signaling through the B cell receptor (36–38), CD40 (39), and BAFF (Blys) (40). Bcl-X_L enhances the survival of follicular and germinal center B cells (41), the presumed targets of the misguided DNA double-strand-break repair that generates chromosomal translocations including those involving *Myc* (42) in B cells undergoing V(D)J hypermutation (43) and isotype switching (44). Bcl-X_L attenuates many death signals, resulting in the rescue of B cells that would normally be eliminated because of aberrant Ig gene rearrangements (31), autoreactivity (45), impaired affinity maturation (46), and genetic defects (47–50). Bcl-X_L also mitigates Myc-dependent apoptosis in B cells, an important mechanism of Myc-induced lymphomagenesis (51). Targeting Bcl-X_L expression to mature B and plasma cells might thus promote the neoplastic transformation of plasma cells, specifically those harboring *Myc*-activating chromosomal translocations or genetically engineered mutations that mimic such translocations in the germ line.

To test the possibility that deregulation of Myc and Bcl-X_L in plasma cells might result in plasma cell tumors in mice, we developed two transgenic mouse strains. The first strain harbors a histidine-tagged mouse *Myc* gene, Myc^{His}, inserted into the Cα gene of an otherwise intact mouse *Igh* locus that contains Eμ, Eα, and all other regulatory elements residing in the *Igh* (Myc transgenics). The inserted *Myc* mimics the *Myc*-activating chromosomal T(12;15) translocation most commonly observed in peritoneal PCT of BALB/c mice. The second strain contains a multicopy Flag-tagged mouse $Bcl\text{-}x^{Flag}$ transgene driven by the mouse Ig κ light-chain 3′ enhancer (Bcl-X_L transgenics). This transgene effects constitutive expression of Bcl-X_L, the major splice form of *Bcl-x* mRNA, in B cells and plasma cells. Here we show that single-transgenic Myc and Bcl-X_L mice exhibit moderate phenotypes with little or no impact on tumor development and lifespan of mice. In sharp contrast, double-transgenic Myc/Bcl-X_L mice develop plasma cell tumors rapidly (135 days mean onset) and with full penetrance (100% tumor incidence). Our results show that novel targeted deregulation of Myc and Bcl-X_L leads to a mouse model of human PCN that may be useful to elucidate the mechanism of the Myc/Bcl-X_L collaboration and to design new approaches for treatment and prevention of human PCN.

Methods

Generation of Myc transgenics. Gene targeting (52) and cre-loxP recombination (53) were used to insert a mouse *Myc* gene into the mouse germ-line *Igh* locus (Figure 1A). The inserted *Myc* consisted of an intron-less cDNA clone, the noncoding first exon with the natural P1/P2 promoter, 1.5 kb of genomic 5′ flank containing the normal transcription-regulatory region, and a short stretch of 3′ untranslated region (UTR) harboring the *Myc* major polyadenylation site. The UTR 3′ of the polyadenylation signal, which has been shown to be dispensable in vivo (54), was not present in the construct. The *Myc* coding region also contained an artificial histidine tag added in frame at its 3′ end. The tag made it possible to distinguish *Myc* mRNA and Myc protein encoded by the inserted Myc^{His} gene from message and protein encoded by the normal, endogenous *Myc* gene. Myc^{His} was inserted in opposite transcriptional orientation in intron 1 of the Cα locus. The construction of the inserted *Myc*, referred to as $iMyc^{Cα}$, the assembly of the targeting vector, and the generation of the transgenic mice are described in the Supplemental Methods section and illustrated in Supplemental Figure 1 (suplemental material available at http://www.jci.org/cgi/content/full/113/12/1763/DC1). The Myc transgenic mice were of mixed C57BL/6 × 129SvJ background (Figure 1C).

Generation of Bcl-X_L transgenics. Injection of plasmid DNA into male pronuclei of FVB/N zygotes was used to generate the Bcl-X_L transgenic mice (Figure 1B). The transgene, referred to as 3′KE-Bcl-X_L, was a modification of a previously developed *Bcl-x* transgene developed by Tim Behrens (University of Minnesota, Minneapolis, Minnesota, USA) (31). It contains the same $Bcl\text{-}x^{Flag}$ gene but uses the 3′ κ enhancer and V_K21 promoter (excised from plasmid K3′E.KP.LUC; ref. 55) in place of the intronic Eμ enhancer and TK promoter to drive *Bcl-x* expression. Prior to microinjection, plasmid 3′κE-Bcl-x_L was purified by cesium chloride centrifugation and linearized by digestion with NotI/AseI.

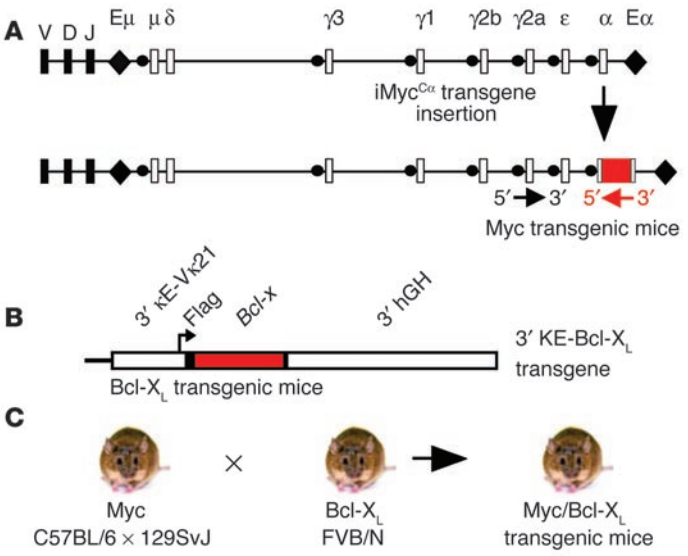

Figure 1
Experimental overview of the generation of double-transgenic Myc/Bcl-X_L mice. (**A**) Generation of Myc transgenic mice. Shown are the normal mouse *Igh* locus (top) and the targeted *Igh* locus with the inserted Myc^{His} gene (bottom). The transcriptional orientation of *Igh* and Myc^{His} is indicated by a black and a red arrow, respectively. (**B**) Generation of Bcl-X_L transgenic mice. Depicted is a scheme of the *Bcl-x* transgene, which consists of the mouse 3′ κ enhancer; the promoter of the mouse variable κ gene, Vκ21; the mouse *Bcl-x* cDNA fused to the Flag epitope–encoding sequence; and the 3′ untranslated region of the human growth hormone (3′ hGH), a facilitator of *Bcl-x* expression. (**C**) Myc/Bcl-X_L bitransgenics were on a mixed genetic background containing alleles from strains C57BL/6, 129SvJ, and FVB/N.

Data presented in this report were collected using animals from the founder line 1967 (56). The Bcl-X_L transgenic mice were of inbred FVB/N background (Figure 1C).

Generation of double-transgenic Myc/Bcl-X_L mice. Hemizygous Myc transgenic mice were crossed with hemizygous Bcl-X_L transgenic mice to generate bitransgenics, which were born at the expected frequency of approximately 25%. The bitransgenic mice, henceforth referred to as Myc/Bcl-X_L mice, were of mixed C57BL/6 × 129SvJ × FVB/N background (Figure 1C). Single-transgenic Myc and Bcl-X_L F_1 progeny (~50% of offspring in the above-mentioned cross) and nontransgenic F_1 progeny (~25% of offspring) were used as controls unless otherwise noted. Breeding and maintenance of mice and all experimentation involving mice were approved under Institutional Animal Care and Use Committee Protocol 0006A56361 (University of Minnesota) and Animal Study Protocol LG-028 (National Cancer Institute [NCI]).

Histology and immunohistochemistry. Tissues were fixed overnight in 10% buffered formalin and embedded in paraffin. Deparaffinized tissue sections were stained with H&E for histological examination by light microscopy or left unstained for marker analysis by immunohistochemistry. The latter involved incubation with biotin-conjugated antibodies to mouse B220 (RA3-6B2), CD138 (281-2; both from BD Biosciences, San Jose, California, USA), and Igκ (Southern Biotechnology Associates Inc., Birmingham, Alabama, USA), or incubation with unlabeled antibodies from rabbit to mouse phosphohistone H3 (Ser10) and cleaved caspase-3 (Asp175; both from Cell Signaling Technology Inc., Beverly, Massachusetts, USA) followed by a labeled secondary, goat anti-rabbit antibody. Antibody binding in tissue sections was visualized by the VECTASTAIN ABC alkaline phosphatase kit or the ABC peroxidase kit (Vector Laboratories Inc., Burlingame, California, USA) using Vector Blue or NovaRED as substrates. Endogenous alkaline phosphatase and peroxidase activities were inhibited by levamisole and hydrogen peroxide, respectively. Tissue sections were counterstained with hematoxylin.

ELISA. Serum IgG and IgM concentrations were measured by ELISA using capture antibodies binding to both heavy chains and light chains (2 μg/ml; Caltag Laboratories Inc., Burlingame, California, USA). BSA (1%) was used for blocking. Serial dilutions of serum samples (1:2,000, 1:10,000, 1:50,000, 1:250,000, 1:500,000) were incubated at 4°C overnight in coated ELISA plates. Individual isotypes (IgG1, IgG2a, IgG2b, IgG3, and IgM) were detected with the help of biotinylated goat anti-mouse antibodies (Caltag Laboratories Inc.), followed by binding to alkaline phosphatase–conjugated streptavidin (Caltag Laboratories Inc.) and addition of 1 mg/ml alkaline phosphatase substrate in diethanolamine buffer. The optical densities were measured at 405 nm using a microplate reader.

Flow cytometry and cell sorting. To determine subpopulations of lymphocytes in mouse tissues, single-cell suspensions from bone marrow, spleen, lymph nodes, and tumors were treated with FcBlock (anti–CD16/CD32, 2.4G2) and directly stained with mAb's to mouse B220 (RA3-6B2), CD138 (281-2), CD3 (17A2), or IgM (II/41; all from BD Biosciences). These antibodies were conjugated to FITC, phycoerythrin (PE), allophycocyanin, or biotin. Isotype-specific controls demonstrated the specificity of labeling. To estimate the proliferation of normal B and plasma cells from spleen and bone marrow as well neoplastic plasma cells from plasma cell tumors, BrdU incorporation was measured in vitro according to the manufacturer's protocol (BD Biosciences). Forty-eight hours after intraperitoneal injection of 0.5 mg BrdU, the cells were stained with allophycocyanin-labeled anti-B220 and PE-labeled anti-CD138 antibodies, fixed, permeabilized, treated with DNase, and incubated with a FITC-labeled antibody to BrdU. To analyze cell cycling in B and plasma cells, the cells were stained with 50 μg/ml propidium iodide (PI) in the presence of 0.1% sodium citrate and 0.1% Triton X-100. To determine rates of programmed cell death in B cells and plasma cells, the FITC-conjugated monoclonal active caspase-3 antibody apoptosis kit I from BD Biosciences was used (catalog number 550480). In all experiments, cells were analyzed on a Beckman Coulter FC 500 and sorted on an EPICS ALTRA (Beckman Coulter Inc., Fullerton, California, USA).

Cell sorting with magnetic beads (MACS). To determine proliferation and apoptosis in B splenocytes, the MACS mouse B cell sorting kit with B220 beads (Miltenyi Biotec Inc., Auburn, California, USA) was used to purify $B220^+$ cells. Briefly, spleen cells freed of red blood cells were separated on MACS VS+ columns using magnetic beads conjugated to an antibody to mouse B220 (CD45R). Recovery of B cells from single-cell suspensions was approximately 35%. The remaining cells were either $B220^-$ (~35%) or lost (~30%) during cell separation. The purity of MACS-sorted $B220^+$ splenocytes was greater than 90%, as determined by FACS analysis.

Immunoblotting. Proteins from clarified lysates of FACS-sorted homogenized cells from spleen, bone marrow, and plasma cell tumors were resolved electrophoretically in denaturing 10% SDS-PAGE gels and transferred by electroblotting to nitrocellulose membranes. Membranes were probed with rabbit anti-mouse antibodies to histidine tag (Cell Signaling Technology Inc.) and Flag tag (Sigma-Aldrich, St. Louis, Missouri, USA), or rabbit anti-mouse antibodies to cyclin D2 (sc-593), cyclin D1 (sc-717), and XBP-1 (sc-7160) from Santa Cruz Biotechnology Inc. (Santa Cruz, California, USA). The positions of the Myc^{His} and Bcl-x_L^{Flag} proteins were visualized using the Phototope-HRP detection system (Cell Signaling Technology Inc.). To confirm equal loading, the membranes were stripped and reprobed using an antibody specific for actin (CLONTECH Laboratories Inc., Palo Alto, California, USA).

Southern analysis. Genomic DNA (20 μg) was digested with BamHI and EcoRI, fractionated on a 0.7% agarose gel, transferred to a nylon membrane, and crosslinked under UV light. Following prehybridization (Hybrisol I; Intergen, Gaithersburg, Maryland, USA) at 42°C, the membrane was hybridized to a 1.1-kb Cκ probe labeled with ^{32}P-CTP using a random-priming kit. The probe was generated by PCR using a primer pair that was designed by Michael Kuehl (NCI, NIH): 5′-GATGCTGCACCAACTGTATCCA-3′ and 5′-GGGGTGATCAGCTCTCAG-CTT-3′.

Paraproteins. Paraproteins (M-spikes, extragradients) were detected using the Paragon SPE electrophoresis kit (Beckman Coulter Inc.). Ig isotypes were determined by ELISA using Immulon 2 plates (DYNEX Technologies Inc., Chantilly, Virginia, USA) and isotype-specific goat anti-mouse serum labeled with HRP (Southern Biotechnology Associates Inc.). Mouse serum samples were diluted from 10^{-3} to 1.28×10^{-5}. Plates were read on a Molecular Dynamics (Sunnyvale, California, USA) microplate reader at 450 nm.

DNA sequencing of 3′ VDJ regions. The DNA sequence downstream of rearranged variable (V), diversity (D), and joining (J) gene segments of the *Igh* locus was determined as described elsewhere (57). DNA was amplified by PCR using a 5′ primer for the third framework region of VHJ558 genes and a 3′ primer that annealed 400 nucleotides downstream of the JH4 gene segment. The sequences of the forward and reverse primers used for tumor clones were 5′-AGCCTG-ACATCTGAGGAC-3′ and 5′-TAGTGT-

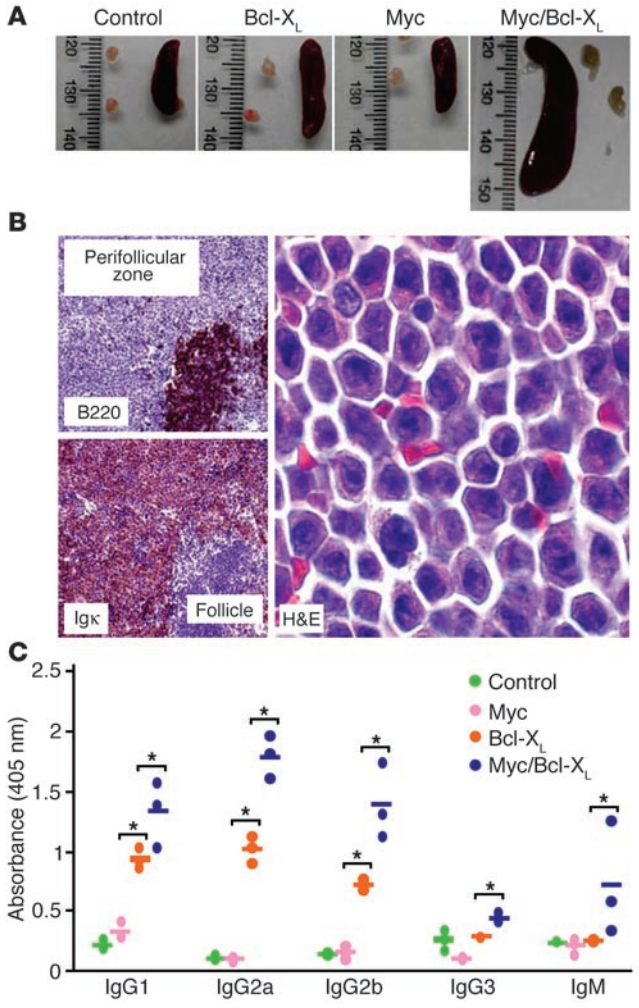

Figure 2
Plasmacytosis and hypergammaglobulinemia in tumor-free Myc/Bcl-X_L transgenic mice. (**A**) Splenomegaly in double-transgenic Myc/Bcl-X_L mice relative to age-matched single-transgenic Myc and Bcl-X_L mice and nontransgenic littermate controls. (**B**) Massive accumulation of plasmablasts and plasma cells in extrafollicular areas of the spleen in Myc/Bcl-X_L transgenics. Left: Low-power view of follicular B cells (top) and plasma cells immunostained for B220 and κ light-chain expression, respectively (original magnification, ×4). Right: High-power view of plasmablasts and plasma cells stained with H&E (original magnification, ×63). (**C**) Marked elevation of serum Ig's in Myc/Bcl-X_L transgenic mice, measured by ELISA. *Significant difference ($P < 0.05$) by Student's *t* test.

GGAACATTCCTCAC-3′, respectively. PCR amplification conditions were 95°C for 0.5 minutes, 63°C for 0.5 minutes, and 72°C for 1.5 minutes for 35 cycles. The sequences of the forward and reverse primers used for plasmablast clones (controls) were 5′-TTTGAATTCCTGACATCTGAGGACTCTGC-3′ and 5′-TTTGGATCCCTCCACCAGACCTCTCTAGA-3′, respectively. PCR conditions were 95°C for 0.5 minutes, 60°C for 0.5 minutes, and 72°C for 1.5 minutes for 30 cycles. PCR products from tumors were sequenced directly, and PCR products from controls were sequenced after cloning into pBluescript (Stratagene, La Jolla, California, USA) at the DNA sequencing facility of Iowa State University (Ames, Iowa, USA). An internal JH4 sequencing primer, iJH4 (5′-CTCCACCAGACCTCTCTAGA-3′), was used in either case.

Results

Features of single-transgenic Myc and Bcl-X_L mice. Myc transgenic mice were generated to recreate and study the molecular and cellular consequences of the *Myc*-activating T(12;15) translocations that characterize BALB/c PCT (Figure 1A). Several noteworthy features of the newly developed mouse strain suggest that insertion of Myc^{His} into *Igh* resulted in representative modeling of T(12;15). First is the precise reconstruction of the translocation breakpoint region on mouse der(12); i.e., the 5′-to-5′ juxtaposition of Myc^{His} and Cα. Second is the potential for Myc^{His} to interact with the complete set of correctly spaced Eα enhancers, designed to create the same complex interplay of promoter and enhancer interactions that govern the expression of translocated *Myc* in mouse PCT. Third is the insertion of Myc^{His} in the *Igh* chromatin domain, which presumably subjects the gene to the same higher-order regulatory influences (e.g., those imposed by chromatin remodeling and positional effects in the interphase nucleus) that affect *Myc* involved in the T(12;15) exchange. Bcl-X_L mice were generated as part of a program to elucidate in transgenic mice the oncogenic properties of death suppressor genes that are frequently overexpressed in human MM (Figure 1B). The *Bcl-x* transgene is a modification of a previously developed *Bcl-x* transgene (31) in which the intronic heavy-chain enhancer Eμ was substituted with the 3′ κ enhancer (56). Compared with Eμ, the 3′ κ enhancer delays $Bcl\text{-}X_L^{Flag}$ expression during B cell development to the mature B cell and plasma cell stage (58), possibly favoring plasma cell tumor formation over B lymphoma development.

Plasmacytosis and hypergammaglobulinemia in double-transgenic Myc/Bcl-X_L mice. Enforced expression of *Myc* and *Bcl-x* by transcriptional control elements with peak activity in plasma cells (3′ Cα and 3′ κ enhancers) might result in expansion of plasma cells in vivo (plasmacytosis). To evaluate this possibility, four 8-week-old Myc/Bcl-X_L mice (Figure 1C) were necropsied, and then lymphoid tissues were examined histologically and immunohistochemically. Four age-matched Myc transgenic mice, Bcl-X_L transgenic mice, and nontransgenic littermates were used as controls. Myc/Bcl-X_L transgenic mice invariably exhibited splenomegaly (Figure 2A), which was mainly caused by the massive accumulation of plasma cells in extrafollicular areas (Figure 2B). Immunostaining of tissue sections for B220 and κ light-chain expression, analogous to the sections shown in Figure 2B, demonstrated that the plasmacytosis sometimes involved nonlymphoid tissues, such as liver (Supplemental Figure 2). The increased tissue load with plasma cells was accompanied by a marked elevation of serum IgM and IgG in the Myc/Bcl-X_L transgenic mice (Figure 2C). Bcl-X_L transgenic mice also exhibited increases in serum Ig, but these were more moderate than in Myc/Bcl-X_L transgenic mice and limited to three IgG isotypes (IgG3 was not higher in Bcl-X_L mice than in Myc and normal mice). Myc transgenic mice were indistinguishable from normal mice (Figure 2C). ELISPOT analysis confirmed the ELISA results. It demonstrated a considerable increase in the number of antibody-producing cells in spleen and bone marrow of Myc/Bcl-X_L transgenic mice compared with single-transgenic Myc and Bcl-X_L mice and normal mice (Supplemental Figure 3a). Plasma cells obtained from tissues with plasmacytosis were

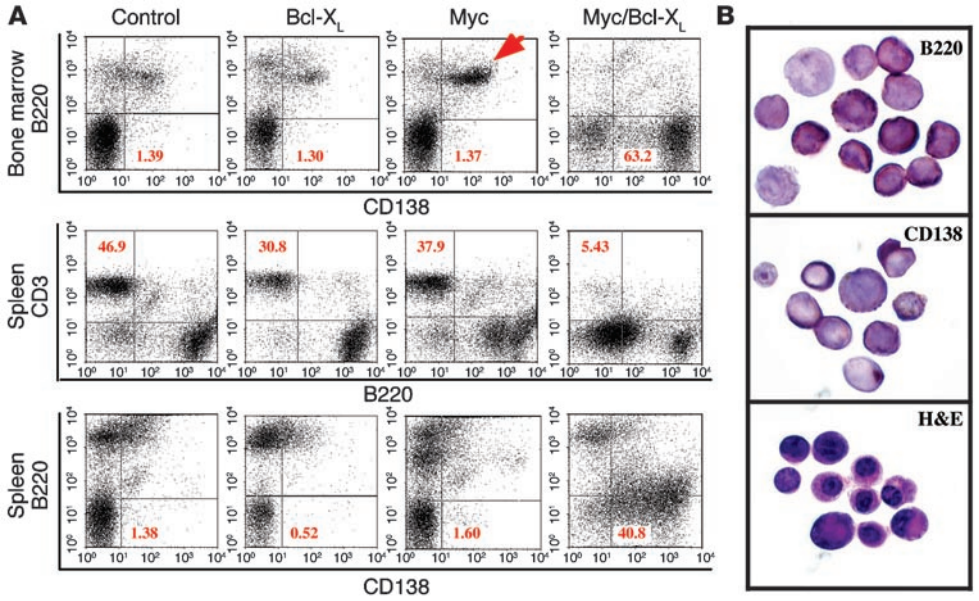

Figure 3
Plasmacytosis in Myc/Bcl-X_L transgenic mice. (**A**) The percentage of B220$^-$CD138$^+$ plasma cells in the bone marrow (top row) and the spleen (bottom row) is indicated in the lower right quadrants of the depicted FACS scatter plots. The percentage of B220$^-$CD3$^+$ T cells in the spleen (center row) is indicated in the upper left quadrants. The red arrow denotes a population of B220$^+$CD138$^+$ plasmablasts in the bone marrow of Myc transgenic mice. (**B**) FACS-sorted B220$^+$CD138$^+$ cells from the bone marrow of Myc transgenic mice express B220 (top), CD138 (center), and Igκ (not shown) by immunostaining and exhibit cytological features of plasmablasts and plasma cells by H&E staining (bottom; original magnification, ×63).

not transplantable into pristane-primed BALB/c nude mice, suggesting that these cells had not yet undergone malignant transformation (Supplemental Figure 3b).

Bcl-X_L promotes survival of Myc^{His}-harboring plasmablasts. To better quantify the apparent expansion of plasma cells in Myc/Bcl-X_L transgenic mice, FACS analysis of bone marrow cells and splenocytes was performed. Six- to 10-week-old bitransgenics were compared with six age-matched single-transgenics and normal mice. Representative examples of each strain are shown in Figure 3A. Myc/Bcl-X_L transgenic mice harbored up to 63% (average 42%, minimum 19%) B220$^-$CD138^{hi} plasma cells in the bone marrow, a striking increase compared with the Myc transgenics, Bcl-X_L transgenics, and normal mice (Figure 3A, top). Similarly, Myc/Bcl-X_L spleen contained up to 57% plasma cells (average 34%, minimum 14%), whereas spleen from the Myc transgenic, Bcl-X_L transgenic, and normal mice contained less than 2% plasma cells (Figure 3A, bottom). Although the relative number of B220$^-$CD3$^+$ T cells was reduced in spleen from Myc/Bcl-X_L bitransgenics compared with the other strains (Figure 3A, center), the absolute number of T cells remained comparable (because of the splenomegaly of strain Myc/Bcl-X_L). Thus, neither transgene by itself, nor the combination of both transgenes grossly interfered with T cell homeostasis in the spleen. Studies with lymph nodes and bone marrow confirmed this observation (results not shown). A special feature of the Myc transgenic mice relative to all other mice was the presence of a distinct population of B220^{hi}CD138$^+$ cells in the bone marrow (22.5% in the example shown in the top panel of Figure 3A). Although the nature of these cells has not been fully elucidated, they likely represent plasmablasts (Figure 3B). The presence of expanded populations of plasmablasts in the Myc mice and plasma cells in the Myc/Bcl-X_L mice suggested that most plasmablasts harboring only deregulated Myc fail to undergo terminal differentiation. However, when protected by Bcl-X_L, Myc transgenic plasmablasts survive and mature into plasma cells.

Increased turnover of Myc-harboring B cells is reduced by Bcl-X_L. *Myc*'s potential to induce proliferation can be mitigated in vivo by *Myc*'s ability to trigger apoptosis (59). To compare proliferation and apoptosis in mature B cells of Myc/Bcl-X_L bitransgenic mice with those in single-transgenic Myc and Bcl-X_L mice and nontransgenic littermates, tissue sections of lymph nodes from 8-week-old mice were immunostained with antibody to phosphohistone H3 (a marker of mitosis) and cleaved caspase-3 (a marker of apoptosis). B cell proliferation in lymph nodes, predominantly in follicles and germinal centers, was most vigorous in Myc transgenic mice, followed by Myc/Bcl-X_L transgenic, normal, and Bcl-X_L transgenic mice, which had the lowest (Figure 4). To better evaluate the apparent increase in *Myc*-dependent proliferation, FACS analysis of PI-stained cells was combined with BrdU labeling in vivo. *Myc*-harboring B cells proliferated nearly 2.5 times faster by PI staining (Supplemental Figure 4a, left) and three times faster by PI/BrdU staining (Supplemental Figure 4a, center) than the controls. Apoptosis in B cells measured by immunostaining for cleaved caspase-3 was also highest in Myc transgenic mice, lowest in Bcl-X_L transgenic mice, and intermediate in Myc/Bcl-X_L and normal mice (Figure 4). TUNEL of lymph node, spleen, and bone marrow sections confirmed this result (not shown). To better assess the apparent increase in *Myc*-dependent apoptosis, freshly isolated *Myc*-harboring B cells were analyzed by FACS for activation of caspase-3. Apoptosis in these B cells was elevated approximately 4.5-fold compared with normal B cells (Supplemental Figure 4a, right). The propensity of *Myc*-containing B cells to undergo apoptosis was further increased (about twofold) upon activation of cells in vitro with LPS, anti-IgM, or both (Supplemental Figure 4b). Together, these findings indicated that the high turnover of B cells in the Myc transgenic mice is attenuated by Bcl-X_L.

Myc/Bcl-X_L CD138$^+$ cells actively proliferate. Normal plasma cells are end-stage B cells that have lost the ability to proliferate. To evaluate whether plasma cells of Myc/Bcl-X_L transgenic mice adhered to this rule, immunostaining of tissue sections for phosphorylated histone H3 was combined with immunostaining for syndecan-1 (CD138, a marker for plasmablasts and plasma cells) or B220 (CD45, a pan–B cell marker). Doubly stained spleen sections from 8-week-old mice clearly showed that CD138$^+$ cells participated in cell cycling (Supplemental Figure 5a, left). The same result was obtained with

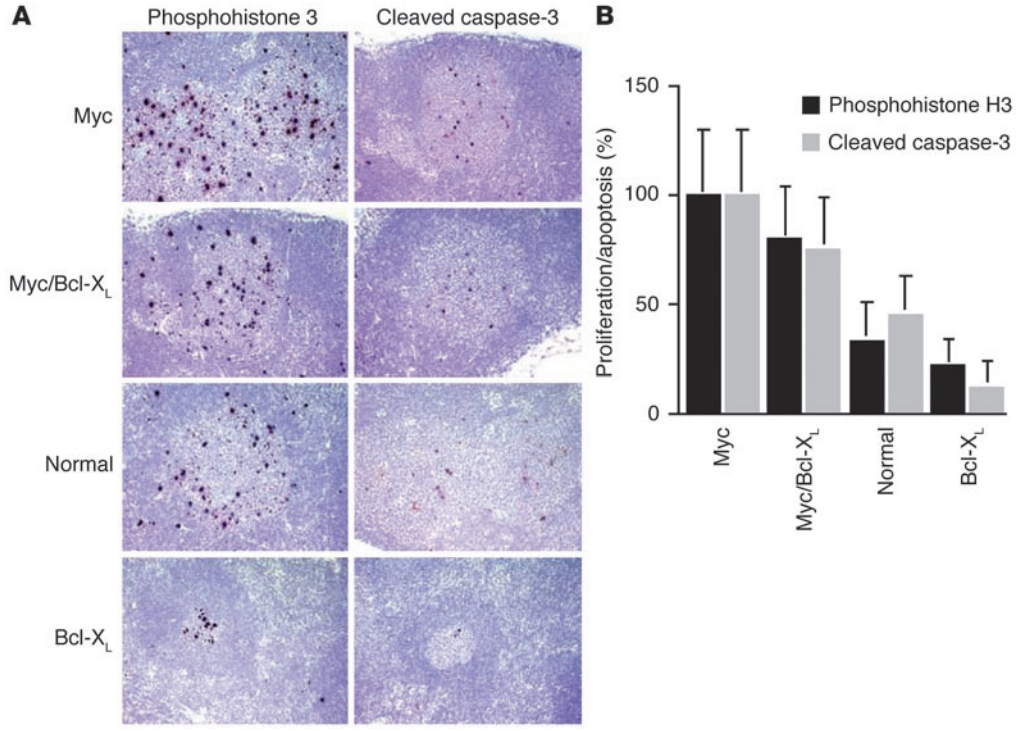

Figure 4
Proliferation and apoptosis in lymph node follicles of 8-week-old Myc, Myc/Bcl-X_L, and Bcl-X_L mice compared with normal nontransgenic littermates. (**A**) Sections of a peripheral lymph node containing two follicles. Follicular B cells undergoing proliferation or apoptosis are immunostained (brown spots) for phosphohistone H3 or activated caspase-3, respectively (original magnification, ×40). The images are ordered from top to bottom according to the apparent turnover of follicular B cells, which was highest in the Myc mice and lowest in the Bcl-X_L mice. (**B**) The result of the microscopic enumeration of proliferating B cells (black bars) and dying B cells (gray bars) in lymph node follicles. Three lymph nodes of each mouse strain were evaluated to determine mean values and SDs of the mean.

lymph node and bone marrow sections (not shown), and when BrdU incorporation in vivo was used as the indicator of proliferation instead of phosphorylated histone H3 (not shown). Double staining of spleen sections (Supplemental Figure 5a, right) or lymph node and bone marrow sections (not shown) for cleaved caspase-3 and CD138 indicated that Myc/Bcl-X_L plasmablasts and plasma cells underwent apoptosis. This observation was confirmed with TUNEL of lymph node, spleen, and bone marrow sections (data not shown). Of importance, the semiquantitative comparison of the extent of proliferation and apoptosis in serial tissue sections of double-transgenic mice, such as those shown in Supplemental Figure 5b, indicated that although there was ongoing apoptosis in Myc/Bcl-X_L CD138$^+$ cells, the balance was tipped in favor of proliferation. This resulted in an enormous expansion of plasma cells, which was unique to the Myc/Bcl-X_L mice and not observed in single-transgenic and control mice. These findings suggested that the interaction of Myc and Bcl-X_L results in an expanded pool of actively proliferating CD138$^+$ cells (most likely plasmablasts) in the double-transgenic mice.

Rapid development of plasma cell tumors in Myc/Bcl-X_L transgenic mice. To evaluate whether the sustained proliferation of Myc/Bcl-X_L plasma cells leads to the development of plasma cell neoplasms, 11 double-transgenic mice were monitored for tumor incidence and survival (Figure 5A). Unlike Bcl-X_L transgenic mice (n = 22) and normal mice (n = 18), which remained tumor free by 380 days of age, Myc/Bcl-X_L mice exhibited a drastically reduced survival. This was caused by malignant plasma cell tumors (Figure 5B) that developed rapidly (mean onset 135 days) and with full penetrance (incidence 100%). *Myc* transgenic mice (n = 43) also developed neoplasms, but tumor development took a long time (mean onset 330 days), occurred with low penetrance (incidence 9.3%), and resulted in B cell lymphomas rather than plasma cell tumors: diffuse large B cell lymphoma in three of four cases (Figure 5A, inset) and unclassified B lymphoma in one case (not shown). The weak tumor phenotype of the Myc mice suggested that although the *Myc*^{His} transgene reproduced the requisite molecular changes that initiate neoplastic B cell and plasma cell development in mice, *Myc*^{His}'s true oncogenic potential in vivo was tempered in the absence of Bcl-X_L.

Features of Myc/Bcl-X_L plasma cell tumors. Plasma cell neoplasms of Myc/Bcl-X_L transgenic mice were CD138$^+$ by immunohistochemistry (Figure 5C), proliferated vigorously by flow cytometry of PI-stained tumor cells (Figure 5C, inset), and expressed transcription factors typical of plasma cells, such as XBP-1 and Blimp-1 message (RT-PCR results not shown) and XBP-1 protein (Figure 5D, top). Immunoblotting showed that Myc/Bcl-X_L tumor cells expressed Myc and Bcl-X_L at higher levels (Figure 5E, lanes 5 and 6) than plasma cells from tumor-free Myc/Bcl-X_L mice (lanes 1 and 8). Flow-sorted tumor cells had a mean Myc^{His}/actin ratio of 2.75 and thus contained 1.8-fold and 2.6-fold higher Myc^{His} protein levels than flow-sorted plasma cells from tumor-free spleen (lane 1) and bone marrow (lane 8), respectively. Consistent with the high Myc level, cyclin D2, a validated Myc target (60), and cyclin D1 were overexpressed in the tumors (Figure 5D, bottom, lanes 1–4) relative to B220$^+$CD138$^+$ plasmablasts from tumor-free Myc/Bcl-X_L mice (control, lane 5). Myc/Bcl-X_L tumors were readily transplantable upon transfer of fewer than 10^6 tumor cells into pristane-primed BALB/c nude mice, with tumor take occurring in less than 2 weeks in two of two cases (not shown). Continuous cell lines were readily derived from two additional cases of primary plasma cell neoplasia. Together, these findings indicated that Myc/Bcl-X_L transgenic mice are predisposed to plasma cell neoplasms that exhibit high levels of Myc^{His} and Bcl-X_L^{Flag} and that have completed malignant transformation.

Origin and distribution of plasma cell tumors. The presentation of Myc/Bcl-X_L transgenic mice with plasma cell tumors in multiple tissues raised the question of whether the tumors originated from a single precursor with the potential for early, widespread

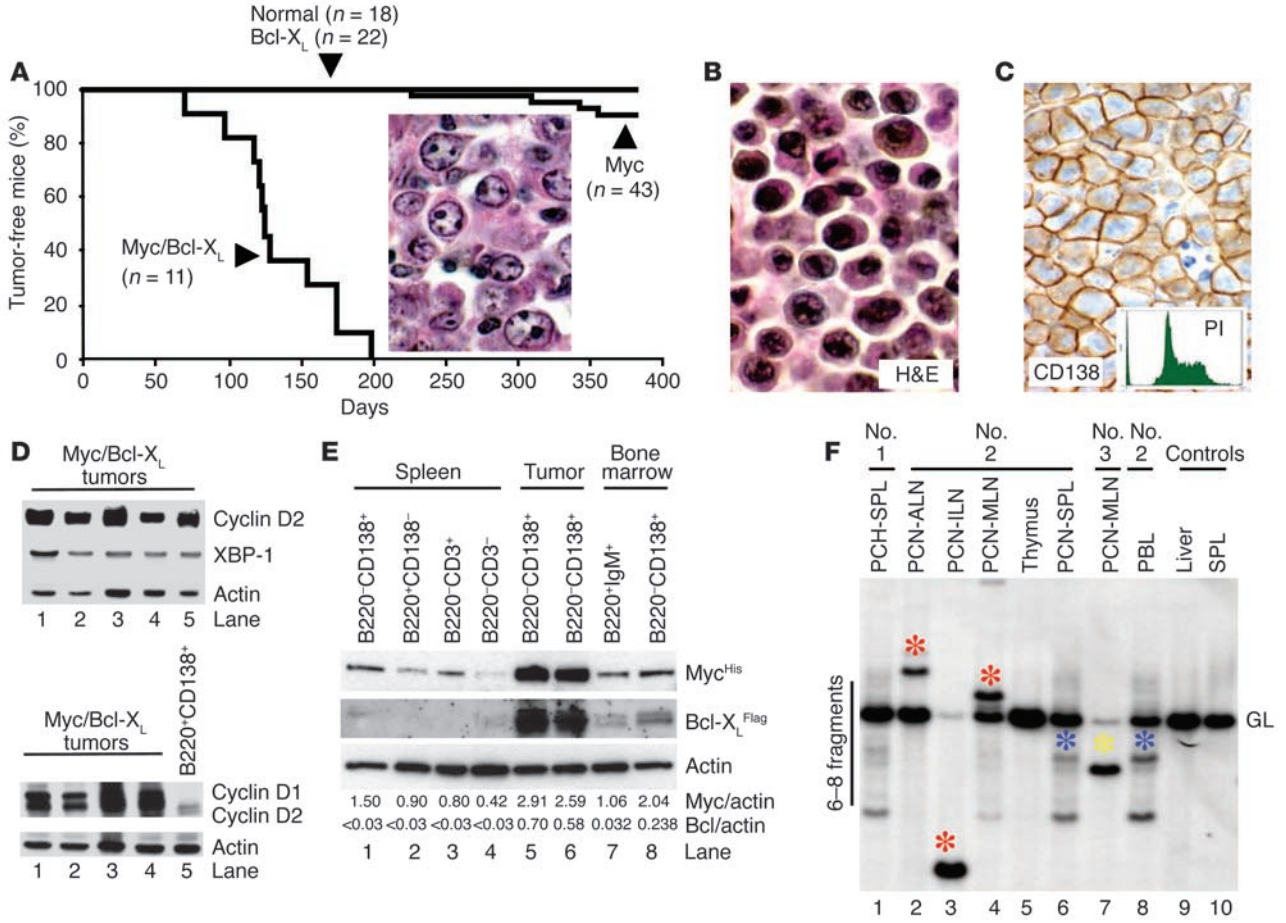

Figure 5
Plasma cell neoplasms in Myc/Bcl-X_L transgenic mice. (**A**) Bcl-X_L transgenic mice (n = 22), nontransgenic littermates (n = 10, not shown), and C57BL/6 mice (n = 18) remained tumor free. Three of four tumors that developed in Myc transgenic mice (n = 43) were diffuse large B cell lymphomas containing abundant neoplastic centroblasts (inset, H&E; original magnification, ×63). (**B**) Typical Myc/Bcl-X_L plasma cell tumor stained with H&E (original magnification, ×63). (**C**) Myc/Bcl-X_L plasma cell neoplasm immunostained for CD138 (brown; original magnification, ×40). The inset shows a FACS profile of the vigorously proliferating propidium iodine–stained tumor cells. (**D**) Western analysis of five Myc/Bcl-X_L plasma cell tumors for expression of cyclin D2 (Myc target), XBP-1 (plasma cell transcription factor), and actin (loading control, top panel). Cyclin D1/D2 expression in Myc/Bcl-X_L plasma cell tumors (lanes 1–4) compared with "premalignant" plasmablasts from tumor-free Myc/Bcl-X_L mice (lane 5, bottom panel). (**E**) Western analysis of Myc^{His} and Bcl-X_L^{Flag} expression in flow-sorted Myc/Bcl-X_L tumor cells (lanes 5–6) compared with cells from spleen (lanes 1–4) and bone marrow (lanes 7–8) of tumor-free Myc/Bcl-X_L mice. Bcl-X_L occurs in two alternative splice forms, with and without transmembrane domain. Myc and Bcl-X_L were detected with antibodies against the histidine and Flag epitopes. (**F**) Southern analysis for clonotypic Igκ rearrangements in PCNs (lanes 2–4, 6, and 7), spleen (SPL) with plasma cell hyperplasia (PCH; lane 1), thymus (lane 5), and peripheral blood leukocytes (PBL; lane 8) from three Myc/Bcl-X_L mice compared with liver and spleen from nontransgenic littermates. ALN, axillary LN; ILN, inguinal LN; MLN, mesenteric LN; GL, germline.

dissemination (monocentric origin), or from multiple precursors resulting in the outgrowth of tumors with different molecular features (multicentric origin). To investigate this, genomic tumor DNA was analyzed by Southern hybridization for clonotypic Igκ rearrangements (Figure 5F). Three different states of tumor dissemination were observed, often coexisting in the same mouse. Some tissues, such as the spleen of mouse no. 1, a borderline case of plasma cell hyper- and neoplasia, harbored multiple clones of aberrant plasma cells (lane 1), reminiscent of the clonal diversity observed in early stages of peritoneal plasmacytomagenesis in BALB/c mice (61). Other tissues, such as the mesenteric lymph node of mouse no. 3 (lane 7), contained one dominant tumor clone (yellow asterisk) that had essentially replaced the normal tissue, as reflected by the loss of the κ germ-line fragment. A third category of tissues, e.g., the lymph nodes in mouse no. 2 (lanes 2–4), harbored different tumor cell clones with distinct κ rearrangements (red asterisks). The detection of an additional cell clone in the peripheral blood leukocyte sample of the same mouse (lane 8, blue asterisk) indicated the emergence of a leukemic clone that had infiltrated the spleen (lane 6) but had not yet reached the thymus (lane 5). These findings reflected a considerable variability in the progression of Myc/Bcl-X_L plasma cell tumors. Some tumors remained confined to lymphoid tissues, where they evolved in mono- or multicentric fashion, whereas other tumors acquired the ability for systemic dissemination, leading to full-blown plasma cell leukemia in some cases (not shown).

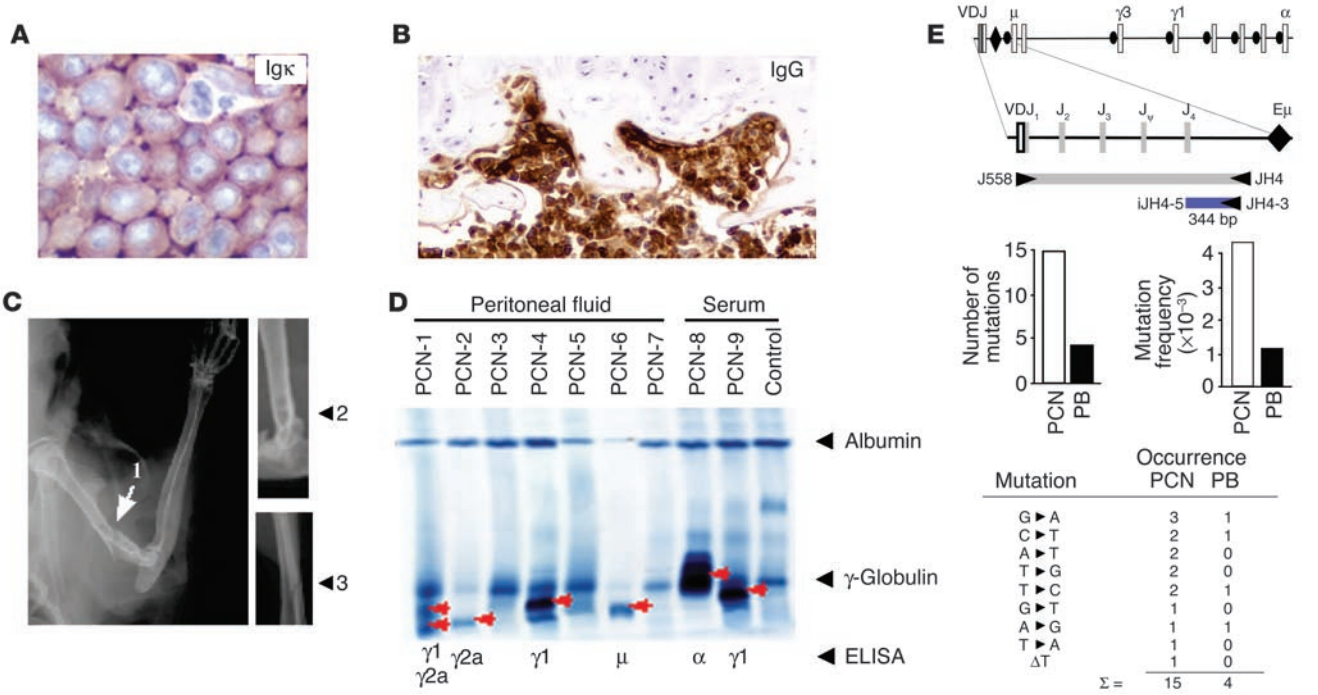

Figure 6
Myc/Bcl-X_L PCNs infiltrate the bone marrow, produce monoclonal Ig, and cause osteolytic lesions. (**A**) Bone marrow infiltration with Igκ-producing neoplastic plasma cells (original magnification, ×63). (**B**) Palisades of neoplastic plasma cells (brown) destroying the luminal face of a femur's corticalis (IgG immunostaining; original magnification, ×40). Two bone resorption lacunae are denoted by arrows. (**C**) Radiographs of large osteolytic lesion with apparent pathological fracture (1, left humerus), osteolytic lesion without fracture (2, right femur), and hairline fracture without visible osteolytic lesion (3, left forearm). (**D**) Protein electropherogram of serum and peritoneal lavage samples containing M-spikes (red arrows) isotyped using ELISA (bottom). (**E**) Frequency and type of mutations in the 3′ JH4 region of rearranged variable (V) genes. Shown at the top is a scheme of the mouse *Igh* locus. PCR primers J558 and JH4 were used to amplify rearranged VDJ genes and linked 3′JH4 sequences. Sequencing primers iJH4-5′ and iJH4-3′ were used to detect mutations in the 344-bp 3′ JH4 region. Shown in the center are bar diagrams of the number of mutations in the 3′ JH4 region in PCNs and plasmablasts from tumor-free Myc/Bcl-X_L mice (PB, left panel). The corresponding mutation frequencies (mutations/3440 bp) are plotted to the right. Shown at the bottom are types and occurrences of base substitution mutations in the 3′ JH4 region of rearranged VH genes in PCN and PB. The tumor sample also contained a deletion, ΔT. The location of the mutation in the 3′ JH4 regions is depicted in Supplemental Figure 6.

Bone marrow involvement of plasma cell tumors. Myc/Bcl-X_L plasma cell tumors demonstrated proclivity to bone marrow involvement, generating coalescent, wall-to-wall tumor masses in several mice with terminal neoplasia (Figure 6A). Histological examination of bone sections from mice with less advanced tumors routinely revealed multifocal lesions of aberrant, pleomorphic plasma cells adjacent to diminished or dissolved osseous trabeculae or located in resorption pits at the inner surface of the corticalis (Figure 6B). Some bone sections contained large sheets of neoplastic plasma cells in soft tissues surrounding the bones, indicating that the tumor had penetrated the corticalis at an obscure, nearby site. Whole-body radiographs showed osteolytic lesions and putative pathological fractures in long bones of three mice (Figure 6C). Serum and peritoneal lavage fluid of tumor-bearing mice often contained monoclonal Ig spikes (extragradients, M components) that were readily detectable by protein electrophoresis (Figure 6D). Two of three tumors from mice without evidence for M-spikes in lavage samples (Figure 6D, lanes 3, 5, and 7) did not express heavy chain (PCN-3) or light chain (PCN-7) by Western analysis (result not shown), possibly because Ig genes were deleted because of genomic instability in the tumors. To determine whether Myc/Bcl-X_L plasma cell tumors exhibit evidence for hypermutation of expressed Ig genes, the 344-bp 3′ JH4 region just downstream of the rearranged VDJ gene was sequenced (Figure 6E, top). Ten tumor-derived clones with unique VH rearrangements were assessed for frequency and type of somatic mutations, and then compared with ten analogous clones from plasmablasts of tumor-free Myc/Bcl-X_L mice (controls). Fifteen mutations were identified in the tumors, and four mutations were found in the plasmablasts ($P = 0.022$, χ^2 analysis; Figure 6E, center left). The corresponding mutation frequencies in the tumors and plasmablasts were 4.36×10^{-3} per bp and 1.16×10^{-3} per bp, respectively (Figure 6E, center right). All mutations except one (a 1-bp deletion) were base substitutions (Figure 6E, bottom). Three mutations in the tumors occurred at WA dinucleotides (W = A or T), a preferred target of the VDJ hypermutation machinery (Supplemental Figure 6). Although these findings are too preliminary for firm conclusions, they suggest that Myc/Bcl-X_L plasma cell tumors have germinal center experience.

Discussion

This study reports the development of a rapid-onset high-penetrance mouse model of human PCN that is based on forced coexpression of Myc and Bcl-X_L in plasma cells. Novel targeted

deregulation of *Myc* (insertion in the proximity of the heavy-chain 3′-Cα enhancer) and *Bcl-x* (activation by the κ light-chain 3′ enhancer) resulted in the formation of transplantable, Ig-producing, CD138$^+$ plasma cell tumors in double-transgenic Myc/Bcl-X_L mice. Tumor development was preceded by massive expansion of normal plasma cells (generalized plasmacytosis) admixed with atypical, dividing plasmablasts (plasma cell hyperplasia), the possible targets of the combined oncogenic attack of Myc and Bcl-X_L. The striking tumor phenotype in Myc/Bcl-X_L bitransgenics — relative to the weak tumor phenotype in single-transgenic Myc mice and the apparent absence of tumors in single-transgenic Bcl-X_L mice — demonstrated that complementation of a proliferation-inducing oncogene (*Myc*) with a death suppressor gene (*Bcl-x*) can greatly accelerate plasma cell neoplasms in mice. This finding was consistent with previous studies on plasmacytomagenesis in mice and recent insights into the biology of Myc and Bcl-X_L in B cells and plasma cells in humans and mice.

The weak oncogenic potency of *Myc*^{His}, on its own, was somewhat surprising. It was probably caused by *Myc*-dependent apoptosis of tumor precursors, rather than failure of the transgenic construct to recreate the biological features of the *Myc*-activating T(12;15) translocation seen in BALB/c PCT. Studies on *Myc* and PCT development in BALB/c mice support this contention. Although, normally, *Myc* promotes cell growth and proliferation in the presence of growth factors (62, 63), deregulated *Myc*, in the absence of growth factors, can force quiescent cells into active cell cycle (64, 65) and then trigger apoptosis. *Myc* has been shown to augment apoptosis by suppressing Bcl-X_L (66). *Myc*-induced apoptosis is a safeguard mechanism for eliminating aberrant cells with active *Myc* (67, 68). In agreement with this, PCT induction studies in BALB/c mice have shown that tumor precursors containing activated *Myc* are removed when positive survival signals provided by IL-6 (69, 70) and environmental antigen stimulation (71, 72) are missing or limiting. Likewise, PCR studies on the occurrence of T(12;15) translocations in mice have demonstrated that the majority of T(12;15)-harboring cells do not evolve into PCT (reviewed in ref. 73), presumably because they are eliminated by *Myc*-induced apoptosis. Although the principal target of *Myc*-dependent apoptosis during tumor development is not known, our observations in the Myc/Bcl-X_L model suggest that the *Myc*^{His}-harboring plasmablast is a candidate. Additional studies are warranted to elucidate Bcl-X_L's survival function in *Myc*-activated plasmablasts.

The finding that 11 of 11 Myc/Bcl-X_L bitransgenics developed plasma cell tumors by 200 days of age demonstrated that Bcl-X_L collaborates with Myc to promote neoplastic plasma cell development. Studies on lymphomagenesis in Eμ-Myc transgenic mice (74) have provided intriguing insights concerning the underlying biology of the Myc/Bcl-X_L collaboration. Eμ-Myc–driven B cell tumors appear to depend on abrogation of Myc-induced apoptosis, e.g., by selection for mutants with upregulated expression of Bcl-2–family proteins, such as Bcl-X_L (75). However, the fact that Bcl-X_L attenuates apoptosis does not exclude that Bcl-X_L uses additional mechanisms to accelerate PCT in mice. Bcl-X_L can delay Myc-induced cell cycle entry by interfering with the ability of Myc to downregulate p27 and activate cyclin/cdk complexes (76). Bcl-X_L can exert promutagenic and genome-destabilizing effects by reducing DNA repair efficiency (77), a possible factor in the development of inflammation-induced PCT in BALB/c mice (78–80). Bcl-X_L is involved in bypassing growth factor requirements and resistance to anoikis (death initiated by loss of contact with ECM components) (81), which may be important for the mobilization and systemic dissemination of malignant plasma cells. Finally, as mentioned above, Bcl-X_L may facilitate the terminal differentiation of *Myc*^{His} plasmablasts, which would be in line with Bcl-X_L's differentiation-enhancing properties in B lymphocytes (45, 50). Thus, although the mechanism of the Myc/Bcl-X_L collaboration may be complex, and although differences in *Myc* deregulation between Eμ-Myc mice and *Myc*^{His} mice may further modify this collaboration, the findings in the Eμ-Myc model strongly suggest that protection from *Myc*-induced apoptosis is a critical component of Bcl-X_L's ability to promote plasma cell tumor formation in Myc/Bcl-X_L mice.

Bone marrow infiltration with malignant plasma cells, a consistent feature of neoplasms arising in Myc/Bcl-X_L mice, indicated that further modification of strain Myc/Bcl-X_L might lead to an improved mouse model of human MM. Possible approaches for modeling human MM in Myc/Bcl-X_L transgenic mice involve the transgenic expression of (a) MM progressor genes, such as *ABL*, *FGFR3*, *RAS*, and *WNT*, (b) transcription factors that commit B cells to the plasma cell fate, such as Blimp-1, IRF4, and XBP-1, (c) chemokine receptors that direct plasma cells from lymph node to bone marrow, such as CXCR4, (d) adhesion molecules that mediate the interaction between plasma cells and stroma cells and/or ECM in the bone marrow, such as syndecan-1, VLA-4, and osteoprotegerin, and (e) mediators of bone destruction, such as MIP-1α, RANKL, and DKK1. Considering that human MM occurs predominantly in elderly patients, it may also become important to delay the expression of the *Myc* and *Bcl-x* transgenes, because their inducible expression in aging mice and their constitutive expression in young mice may favor different types of plasma cell tumor. Furthermore, the well-established importance of modifier genes in peritoneal BALB/c PCT (82) suggests that it may also be necessary to introduce the *Myc* and *Bcl-x* transgenes on a genetic background (e.g., DBA/2N) that is resistant to peritoneal (extramedullary) PCT and, therefore, possibly more conducive to plasma cell tumor formation in the bone marrow.

In conclusion, the remarkable efficiency with which Bcl-X_L synergizes with Myc in plasma cell tumor development in mice extends studies by other investigators who have used Bcl-X_L to promote Myc-dependent oncogenesis in pancreas (59), skin, and other tissues (83). It further extends work with two independently developed Bcl-2 transgenes that facilitated the malignant transformation of B cells and plasma cells harboring deregulated *Myc* (84, 85). Plasma cell tumors in Myc/Bcl-X_L transgenics may afford a good model system for studying the mechanism by which overexpression of Myc and Bcl-X_L facilitates human PCN. It would be particularly interesting to elucidate whether the known mechanisms of Myc enhancement at the transcriptional level (NF-κB [ref. 86] and Stat3 [ref. 87]) and/or the protein level (Ras [ref. 13], NF-κB [ref. 14], and CK2 signaling [ref. 15]) are also operational in the Myc/Bcl-X_L plasma cell tumor model. This information and other insights gleaned from Myc/Bcl-X_L mice may lead to new interventions to inhibit the Myc/Bcl-X_L collaboration for the benefit of the human PCN patient.

Acknowledgments

We wish to thank Lino Tessarollo and Eileen Southon (Gene Targeting Core, NCI) for generating iMyc^{Cα} mice; Sung Sup Park (Korean Research Institute of Bioscience and Biotechnology, Taejon, Republic of Korea) for constructing an early version of the iMyc^{Cα} gene targeting vector; the staff of the Mouse Genetics and Histopathology

Cores, University of Minnesota, for generating and analyzing 3′KE-Bcl-X_L mice; the staff of the mouse facility of the Laboratory of Genetics, Center for Cancer Research (NCI), particularly Wendy DuBois, Lisa Craig, and Vaishali Jarral, for help with the in vivo studies; Sandra Schieferl and Michael Lewis (Cell Signaling Technology Inc.) for outstanding technical assistance; and Michael Comb (Cell Signaling Technology Inc.) and Beverly Mock (NCI) for encouragement and scientific discussion. This study was supported in part by NCI Cancer Biology Training grant T32 CA09138-27 to M. Linden and a grant from the Leukemia Research Fund to B. Van Ness.

Received for publication October 23, 2003, and accepted in revised form April 14, 2004.

Address correspondence to: Siegfried Janz, Laboratory of Genetics, Center for Cancer Research, NCI, Building 37, Room 3140A, Bethesda, Maryland 20892-4256, USA. Phone: (301) 496-2202; Fax: (301) 402-1031; E-mail: sj4s@nih.gov.

Wan Cheung Cheung and Joong Su Kim contributed equally to this work.

1. Radl, J. 1999. Multiple myeloma and related disorders. Lessons from an animal model. *Pathol. Biol. (Paris).* **47**:109–114.
2. Potter, M. 1997. Experimental plasmacytomagenesis in mice. *Hematol. Oncol. Clin. North Am.* **11**:323–347.
3. Yaccoby, S., Barlogie, B., and Epstein, J. 1998. Primary myeloma cells growing in SCID-hu mice: a model for studying the biology and treatment of myeloma and its manifestations. *Blood.* **92**:2908–2913.
4. Yaccoby, S., and Epstein, J. 1999. The proliferative potential of myeloma plasma cells manifest in the SCID-hu host. *Blood.* **94**:3576–3582.
5. Pearse, R.N., et al. 2001. Multiple myeloma disrupts the TRANCE/ osteoprotegerin cytokine axis to trigger bone destruction and promote tumor progression. *Proc. Natl. Acad. Sci. U. S. A.* **98**:11581–11586.
6. Kovalchuk, A.L., et al. 2002. IL-6 transgenic mouse model for extraosseous plasmacytoma. *Proc. Natl. Acad. Sci. U. S. A.* **99**:1509–1514.
7. Chiarle, R., et al. 2003. NPM-ALK transgenic mice spontaneously develop T-cell lymphomas and plasma cell tumors. *Blood.* **101**:1919–1927.
8. Lange, K., et al. 2003. Overexpression of NPM-ALK induces different types of malignant lymphomas in IL-9 transgenic mice. *Oncogene.* **22**:517–527.
9. De Vos, J., et al. 2002. Comparison of gene expression profiling between malignant and normal plasma cells with oligonucleotide arrays. *Oncogene.* **21**:6848–6857.
10. Zhan, F., et al. 2002. Global gene expression profiling of multiple myeloma, monoclonal gammopathy of undetermined significance, and normal bone marrow plasma cells. *Blood.* **99**:1745–1757.
11. Kiuchi, N., et al. 1999. STAT3 is required for the gp130-mediated full activation of the c-myc gene. *J. Exp. Med.* **189**:63–73.
12. Chappell, S.A., et al. 2000. A mutation in the c-myc-IRES leads to enhanced internal ribosome entry in multiple myeloma: a novel mechanism of oncogene de-regulation. *Oncogene.* **19**:4437–4440.
13. Sears, R., Leone, G., DeGregori, J., and Nevins, J.R. 1999. Ras enhances Myc protein stability. *Mol. Cell.* **3**:169–179.
14. Grumont, R.J., Strasser, A., and Gerondakis, S. 2002. B cell growth is controlled by phosphatidylinosotol 3-kinase-dependent induction of Rel/ NF-κB regulated c-myc transcription. *Mol. Cell.* **10**:1283–1294.
15. Channavajhala, P., and Seldin, D.C. 2002. Functional interaction of protein kinase CK2 and c-Myc in lymphomagenesis. *Oncogene.* **21**:5280–5288.
16. Shou, Y., et al. 2000. Diverse karyotypic abnormalities of the c-myc locus associated with c-myc dysregulation and tumor progression in multiple myeloma. *Proc. Natl. Acad. Sci. U. S. A.* **97**:228–233.
17. Avet-Loiseau, H., et al. 2001. Rearrangements of the c-myc oncogene are present in 15% of primary human multiple myeloma tumors. *Blood.* **98**:3082–3086.
18. Fabris, S., et al. 2003. Heterogeneous pattern of chromosomal breakpoints involving the MYC locus in multiple myeloma. *Genes Chromosomes Cancer.* **37**:261–269.
19. Ohno, S., et al. 1979. Nonrandom chromosome changes involving the Ig gene-carrying chromosomes 12 and 6 in pristane-induced mouse plasmacytomas. *Cell.* **18**:1001–1007.
20. Wiener, F., et al. 1984. High resolution banding analysis of the involvement of strain BALB/ c- and AKR-derived chromosomes No. 15 in plasmacytoma-specific translocations. *J. Exp. Med.* **159**:276–291.
21. Shen-Ong, G.L., Keath, E.J., Piccoli, S.P., and Cole, M.D. 1982. Novel myc oncogene RNA from abortive immunoglobulin-gene recombination in mouse plasmacytomas. *Cell.* **31**:443–452.
22. Krajewski, S., et al. 1994. Immunohistochemical analysis of in vivo patterns of Bcl-X expression. *Cancer Res.* **54**:5501–5507.
23. Zhang, B., Gojo, I., and Fenton, R.G. 2002. Myeloid cell factor-1 is a critical survival factor for multiple myeloma. *Blood.* **99**:1885–1893.
24. Spets, H., et al. 2002. Expression of the bcl-2 family of pro- and anti-apoptotic genes in multiple myeloma and normal plasma cells: regulation during interleukin-6(IL-6)-induced growth and survival. *Eur. J. Haematol.* **69**:76–89.
25. Zhang, B., Potyagaylo, V., and Fenton, R.G. 2003. IL-6-independent expression of Mcl-1 in human multiple myeloma. *Oncogene.* **22**:1848–1859.
26. Puthier, D., et al. 1999. Mcl-1 and Bcl-xL are co-regulated by IL-6 in human myeloma cells. *Br. J. Haematol.* **107**:392–395.
27. Tu, Y., et al. 1998. BCL-X expression in multiple myeloma: possible indicator of chemoresistance. *Cancer Res.* **58**:256–262.
28. Gauthier, E.R., Piche, L., Lemieux, G., and Lemieux, R. 1996. Role of bcl-X(L) in the control of apoptosis in murine myeloma cells. *Cancer Res.* **56**:1451–1456.
29. Underhill, G.H., George, D., Bremer, E.G., and Kansas, G.S. 2003. Gene expression profiling reveals a highly specialized genetic program of plasma cells. *Blood.* **101**:4013–4021.
30. Ursini-Siegel, J., et al. 2002. TRAIL/Apo-2 ligand induces primary plasma cell apoptosis. *J. Immunol.* **169**:5505–5513.
31. Fang, W., et al. 1996. Frequent aberrant immunoglobulin gene rearrangements in pro-B cells revealed by a bcl-xL transgene. *Immunity.* **4**:291–299.
32. McDonnell, T.J., et al. 1989. bcl-2-immunoglobulin transgenic mice demonstrate extended B cell survival and follicular lymphoproliferation. *Cell.* **57**:79–88.
33. Strasser, A., et al. 1990. Abnormalities of the immune system induced by dysregulated bcl-2 expression in transgenic mice. *Curr. Top. Microbiol. Immunol.* **166**:175–181.
34. Zhou, P., et al. 2001. MCL1 transgenic mice exhibit a high incidence of B-cell lymphoma manifested as a spectrum of histologic subtypes. *Blood.* **97**:3902–3909.
35. Chuang, P.I., et al. 2002. Perturbation of B-cell development in mice overexpressing the Bcl-2 homolog A1. *Blood.* **99**:3350–3359.
36. Solvason, N., et al. 1996. Induction of cell cycle regulatory proteins in anti-immunoglobulin-stimulated mature B lymphocytes. *J. Exp. Med.* **184**:407–417.
37. Anderson, J.S., Teutsch, M., Dong, Z., and Wortis, H.H. 1996. An essential role for Bruton's tyrosine kinase in the regulation of B-cell apoptosis. *Proc. Natl. Acad. Sci. U. S. A.* **93**:10966–10971.
38. Grumont, R.J., et al. 1998. B lymphocytes differentially use the Rel and nuclear factor kappaB1 (NF-kappaB1) transcription factors to regulate cell cycle progression and apoptosis in quiescent and mitogen-activated cells. *J. Exp. Med.* **187**:663–674.
39. Tuscano, J.M., et al. 1996. Bcl-x rather than Bcl-2 mediates CD40-dependent centrocyte survival in the germinal center. *Blood.* **88**:1359–1364.
40. Do, R.K., et al. 2000. Attenuation of apoptosis underlies B lymphocyte stimulator enhancement of humoral immune response. *J. Exp. Med.* **192**:953–964.
41. Grillot, D.A., et al. 1996. bcl-x exhibits regulated expression during B cell development and activation and modulates lymphocyte survival in transgenic mice. *J. Exp. Med.* **183**:381–391.
42. Kuppers, R., and Dalla-Favera, R. 2001. Mechanisms of chromosomal translocations in B cell lymphomas. *Oncogene.* **20**:5580–5594.
43. Pasqualucci, L., et al. 2001. Hypermutation of multiple proto-oncogenes in B-cell diffuse large-cell lymphomas. *Nature.* **412**:341–346.
44. Nagaoka, H., Muramatsu, M., Yamamura, N., Kinoshita, K., and Honjo, T. 2002. Activation-induced deaminase (AID)-directed hypermutation in the immunoglobulin Smu region: implication of AID involvement in a common step of class switch recombination and somatic hypermutation. *J. Exp. Med.* **195**:529–534.
45. Fang, W., et al. 1998. Self-reactive B lymphocytes overexpressing Bcl-xL escape negative selection and are tolerized by clonal anergy and receptor editing. *Immunity.* **9**:35–45.
46. Takahashi, Y., et al. 1999. Relaxed negative selection in germinal centers and impaired affinity maturation in bcl-xL transgenic mice. *J. Exp. Med.* **190**:399–410.
47. Solvason, N., et al. 1998. Transgene expression of bcl-xL permits anti-immunoglobulin (Ig)-induced proliferation in xid B cells. *J. Exp. Med.* **187**:1081–1091.
48. Owyang, A.M., et al. 2001. c-Rel is required for the protection of B cells from antigen receptor-mediated, but not Fas-mediated, apoptosis. *J. Immunol.* **167**:4948–4956.
49. Suzuki, H., et al. 2003. PI3K and Btk differentially regulate B cell antigen receptor-mediated signal transduction. *Nat. Immunol.* **4**:280–286.
50. Amanna, I.J., Dingwall, J.P., and Hayes, C.E. 2003. Enforced bcl-xL gene expression restored splenic B lymphocyte development in BAFF-R mutant mice. *J. Immunol.* **170**:4593–4600.
51. Eischen, C.M., Woo, D., Roussel, M.F., and Cleveland, J.L. 2001. Apoptosis triggered by Myc-induced suppression of Bcl-X(L) or Bcl-2 is bypassed during lymphomagenesis. *Mol. Cell. Biol.* **21**:5063–5070.
52. Thomas, K.R., and Capecchi, M.R. 1987. Site-directed mutagenesis by gene targeting in mouse embryo-derived stem cells. *Cell.* **51**:503–512.
53. Gu, H., Zou, Y.R., and Rajewsky, K. 1993. Independent control of immunoglobulin switch recombination at individual switch regions evidenced

through Cre-loxP-mediated gene targeting. *Cell.* **73**:1155–1164.
54. Langa, F., et al. 2001. Healthy mice with an altered c-myc gene: role of the 3′ untranslated region revisited. *Oncogene.* **20**:4344–4353.
55. Fulton, R., and Van Ness, B. 1993. Kappa immunoglobulin promoters and enhancers display developmentally controlled interactions. *Nucleic Acids Res.* **21**:4941–4947.
56. Linden, M.A., Kirchhof, N., Carlson, C.S., and Van Ness, B.G. 2004. Targeted overexpression of Bcl-XL in B-lymphoid cells results in lymphoproliferative disease and plasma cell malignancies. *Blood.* **103**:2779–2786.
57. McDonald, J.P., et al. 2003. 129-Derived strains of mice are deficient in DNA polymerase ι and have normal immunoglobulin hypermutation. *J. Exp. Med.* **198**:635–643.
58. Gorman, J.R., and Alt, F.W. 1998. Regulation of immunoglobulin light chain isotype expression. *Adv. Immunol.* **69**:113–181.
59. Pelengaris, S., Khan, M., and Evan, G.I. 2002. Suppression of Myc-induced apoptosis in β cells exposes multiple oncogenic properties of Myc and triggers carcinogenic progression. *Cell.* **109**:321–334.
60. Gomez-Roman, N., Grandori, C., Eisenman, R.N., and White, R.J. 2003. Direct activation of RNA polymerase III transcription by c-Myc. *Nature.* **421**:290–294.
61. Kovalchuk, A.L., Mushinski, E.B., and Janz, S. 2000. Clonal diversification of primary BALB/c plasmacytomas harboring T(12;15) chromosomal translocations. *Leukemia.* **14**:909–921.
62. Eilers, M., Schirm, S., and Bishop, J.M. 1991. The MYC protein activates transcription of the α-prothymosin gene. *EMBO J.* **10**:133–141.
63. Mateyak, M.K., Obaya, A.J., Adachi, S., and Sedivy, J.M. 1997. Phenotypes of c-Myc-deficient rat fibroblasts isolated by targeted homologous recombination. *Cell Growth Differ.* **8**:1039–1048.
64. Prochownik, E.V., Kukowska, J., and Rodgers, C. 1988. c-myc antisense transcripts accelerate differentiation and inhibit G1 progression in murine erythroleukemia cells. *Mol. Cell. Biol.* **8**:3683–3695.
65. Askew, D.S., Ashmun, R.A., Simmons, B.C., and Cleveland, J.L. 1991. Constitutive c-myc expression in an IL-3-dependent myeloid cell line suppresses cell cycle arrest and accelerates apoptosis. *Oncogene.* **6**:1915–1922.
66. Maclean, K.H., Keller, U.B., Rodriguez-Galindo, C., Nilsson, J.A., and Cleveland, J.L. 2003. c-Myc augments γ irradiation-induced apoptosis by suppressing Bcl-XL. *Mol. Cell. Biol.* **23**:7256–7270.
67. Bissonnette, R.P., Echeverri, F., Mahboubi, A., and Green, D.R. 1992. Apoptotic cell death induced by c-myc is inhibited by bcl-2. *Nature.* **359**:552–554.
68. Evan, G.I., et al. 1992. Induction of apoptosis in fibroblasts by c-myc protein. *Cell.* **69**:119–128.
69. Shacter, E., Arzadon, G.K., and Williams, J. 1992. Elevation of interleukin-6 in response to a chronic inflammatory stimulus in mice: inhibition by indomethacin. *Blood.* **80**:194–202.
70. Lattanzio, G., et al. 1997. Defective development of pristane-oil-induced plasmacytomas in interleukin-6-deficient BALB/c mice. *Am. J. Pathol.* **151**:689–696.
71. McIntire, K.R., and Princler, G.L. 1969. Prolonged adjuvant stimulation in germ-free BALB-c mice: development of plasma cell neoplasia. *Immunology.* **17**:481–487.
72. Byrd, L.G., McDonald, A.H., Gold, L.G., and Potter, M. 1991. Specific pathogen-free BALB/cAn mice are refractory to plasmacytoma induction by pristane. *J. Immunol.* **147**:3632–3637.
73. Janz, S., Potter, M., and Rabkin, C.S. 2003. Lymphoma- and leukemia-associated chromosomal translocations in healthy individuals. *Genes Chromosomes Cancer.* **36**:211–223.
74. Adams, J.M., et al. 1985. The c-myc oncogene driven by immunoglobulin enhancers induces lymphoid malignancy in transgenic mice. *Nature.* **318**:533–538.
75. Eischen, C.M., et al. 2001. Bcl-2 is an apoptotic target suppressed by both c-Myc and E2F-1. *Oncogene.* **20**:6983–6993.
76. Greider, C., Chattopadhyay, A., Parkhurst, C., and Yang, E. 2002. BCL-x(L) and BCL2 delay Myc-induced cell cycle entry through elevation of p27 and inhibition of G1 cyclin-dependent kinases. *Oncogene.* **21**:7765–7775.
77. Saintigny, Y., Dumay, A., Lambert, S., and Lopez, B.S. 2001. A novel role for the Bcl-2 protein family: specific suppression of the RAD51 recombination pathway. *EMBO J.* **20**:2596–2607.
78. Sanford, K.K., et al. 1986. Chromosomal radiosensitivity during G2 phase and susceptibility to plasmacytoma induction in mice. *Curr. Top. Microbiol. Immunol.* **132**:202–208.
79. Shacter, E., Lopez, R.L., Beecham, E.J., and Janz, S. 1990. DNA damage induced by phorbol ester-stimulated neutrophils is augmented by extracellular cofactors. Role of histidine and metals. *J. Biol. Chem.* **265**:6693–6699.
80. Beecham, E.J., Mushinski, J.F., Shacter, E., Potter, M., and Bohr, V.A. 1991. DNA repair in the c-myc proto-oncogene locus: possible involvement in susceptibility or resistance to plasmacytoma induction in BALB/c mice. *Mol. Cell. Biol.* **11**:3095–3104.
81. Grad, J.M., Zeng, X.R., and Boise, L.H. 2000. Regulation of Bcl-xL: a little bit of this and a little bit of STAT. *Curr. Opin. Oncol.* **12**:543–549.
82. Zhang, S.L., et al. 2001. Efficiency alleles of the pctr1 modifier locus for plasmacytoma susceptibility. *Mol. Cell. Biol.* **21**:310–318.
83. Pelengaris, S., and Khan, M. 2003. The many faces of c-MYC. *Arch. Biochem. Biophys.* **416**:129–136.
84. McDonnell, T.J., and Korsmeyer, S.J. 1991. Progression from lymphoid hyperplasia to high-grade malignant lymphoma in mice transgenic for the t(14; 18). *Nature.* **349**:254–256.
85. Strasser, A., Harris, A.W., and Cory, S. 1993. E mu-bcl-2 transgene facilitates spontaneous transformation of early pre-B and immunoglobulin-secreting cells but not T cells. *Oncogene.* **8**:1–9.
86. Kanda, K., Hu, H.M., Zhang, L., Grandchamps, J., and Boxer, L.M. 2000. NF-κ B activity is required for the deregulation of c-myc expression by the immunoglobulin heavy chain enhancer. *J. Biol. Chem.* **275**:32338–32346.
87. Noronha, E.J., Sterling, K.H., and Calame, K.L. 2003. Increased expression of Bcl-xL and c-Myc is associated with transformation by Abelson murine leukemia virus. *J. Biol. Chem.* **278**:50915–50922.